ELSEVIER

Palaeogeography, Palaeoclimatology, Palaeoecology 197 (2003) 151–169

PALAEO

www.elsevier.com/locate/palaeo

Geochemical taphonomy of shallow marine vertebrate assemblages

C.N. Trueman [a,*], M.J. Benton [a], M.R. Palmer [b]

[a] *Department of Earth Sciences, University of Bristol, Bristol BS8 1RJ, UK*

[b] *School of Ocean and Earth Sciences, University of Southampton, Southampton Oceanography Centre, European Way, Southampton SO14 3ZH, UK*

Received 26 October 2001; accepted 2 May 2003

Abstract

Combined histological and geochemical analyses demonstrate complex processes leading to preservation of microbially altered bone. In certain situations, a chemical microenvironment distinct from surrounding pore waters is developed and maintained within the bone. The bone acts as a closed system, and hence palaeoenvironmental interpretations based on fossil bone apatite chemistry may not accurately reflect overall geochemical conditions of the sedimentary deposits where the bones were buried. Geochemical techniques based on variance in trace element compositions of bones from different assemblages can be used as a measure of the relative degree of mixing or taphonomic averaging within marine vertebrate assemblages.

Keywords: bones; taphonomy; rare earth elements; diagenesis; redox; marine

1. Introduction

1.1. Background

Many site-specific processes, including the rate of destruction of organic remains and the sedimentation rate, control the length of time taken to form a fossil assemblage (time averaging). Time averaging is important because many taphonomic and taxonomic features of bone assemblages depend on the amount of time over which skeletal remains are accumulated (Behrensmeyer and Hook, 1992). Unfortunately, it is difficult to quantify time averaging in any given fossil-bearing deposit, and this limits inferences that can be drawn from fossil assemblages (see Behrensmeyer et al. (2000) for a recent discussion of time averaging). Trueman and Benton (1997) and Staron et al. (2001) demonstrated that the rare earth element (REE) composition of fossil bones from shallow marine assemblages could be used to test for reworking. Such geochemical taphonomic techniques are built upon the observation that trace metals are incorporated rapidly into bone post mortem, and that the relative abundance of these trace metals in fossil bone reflects, at least

* Corresponding author. Present address: School of Earth and Environmental Sciences, University of Portsmouth, Burnaby Building, Burnaby Road, Portsmouth PO1 3QL, UK.
E-mail address: clive.trueman@port.ac.uk (C.N. Trueman).

0031-0182/03/$ – see front matter © 2003 Elsevier B.V. All rights reserved.
doi:10.1016/S0031-0182(03)00457-7

in part, the microenvironment of burial. Subsequently, Trueman (1999) discussed how variation in the REE content of bones within terrestrial vertebrate assemblages could be used to interpret their accumulation and mixing history. This paper focussed on vertebrate assemblages from terrestrial settings, as the technique exploits variations in the local geochemical environment and such variations are maximised in common terrestrial settings.

The marine environment is relatively homogeneous and buffered geochemically with respect to terrestrial environments. Consequently variations in chemical abundances (e.g. REE patterns) are less varied in marine settings than in terrestrial settings. Any taphonomic techniques based on interpreting variation in geochemical signals will therefore have a lower resolution in marine settings. Nevertheless, geochemical techniques have been used to identify reworked bones in Triassic (Trueman and Benton, 1997) and Cretaceous (Staron et al., 2001) marine bone beds. Traditional taphonomic analyses provide relatively little information for assemblages preserved in marine environments because little is known about the processes of weathering and abrasion in subaqueous marine settings. Consequently, even low-resolution geochemical techniques may contribute significantly to understanding taphonomic processes in marine settings – if they can provide a means for distinguishing different pathways of bone preservation as well as identifying different degrees of time averaging. The trace element geochemistry of shallow marine pore waters is complex, and pore water REE composition varies considerably both in time and space (e.g. Elderfield and Sholkovitz, 1987). This suggests that bones from shallow marine settings with subtly contrasting sedimentary environments may inherit distinct trace metal patterns that could be used as a measure of relative mixing in attritional vertebrate assemblages.

The aim of this paper is firstly to investigate the relationship between recrystallisation and trace element uptake in bones from shallow marine assemblages in order to determine to what extent fossil bone preserves a record of its early depositional environment. Secondly, we attempt to characterise the relationship between sedimentary mixing and geochemical variation in bones from attritional marine vertebrate assemblages.

The major part of the study focuses on material from three marine sample areas: the Upper Triassic (Rhaetian) Westbury Formation of Aust Cliff and Westbury Garden Cliff, Gloucestershire, and the Lower Cretaceous (Berriasian) Broken Shell Member of the Durlston Formation, Durlston Bay, Dorset (Fig. 1). These were chosen as sample areas as the Aust Cliff and Westbury Garden Cliff sites provide two contemporaneous shallow marine siliclastic bone beds with very different taphonmic character. These bone beds can then be compared with the Durlston Bay bone bed that formed in shallow marine carbonate facies. The sedimentology and taphonomy of the Westbury Formation are described in detail by Swift and Martill (1999) and Benton et al. (2002). The sedimentology and palaeoenvironment of the Durlston Formation are discussed by Wright (1996). A brief summary is presented below.

1.2. The Westbury Formation

The Rhaetian stage in Northern Europe is characterised by a rapid transgression separating the terrestrial Mercia Mudstone Group from the marine Lias Group. The Rhaetic transgression forms a major sequence boundary throughout Northern Europe, and is indicated as a major 'Type II Sequence Boundary' on the sea level chart of Haq et al. (1988). In Britain, the Rhaetic transgression consists of a complex sequence of transgressive–regressive cycles, represented by the deposits of the Penarth Group.

In the southwest of England, the Westbury Formation is the lowest unit within the Penarth Group. The Westbury Formation forms a non-sequence boundary within the incipient marine Blue Anchor Formation in low-lying, fault-bounded basins such as the Bristol Channel Basin and the Worcester Graben. During the latest Triassic, structural highs such as the South Wales Massif, Mendip Massif, and Thornbury High stood as land masses or smaller islands within the Westbury seas, and the Westbury Formation

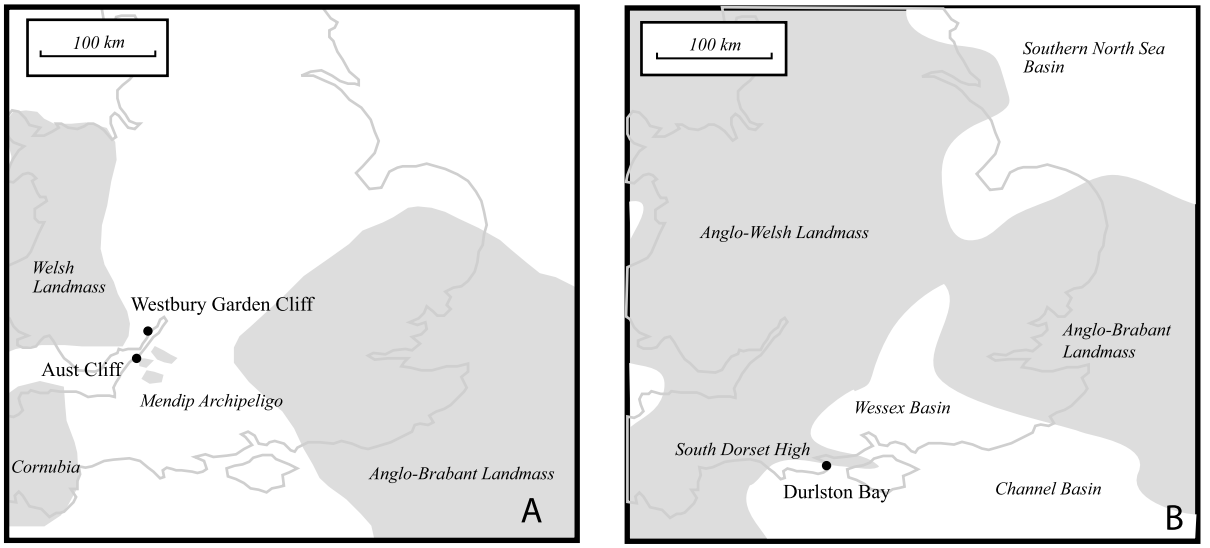

Fig. 1. Palaeogeographic reconstructions of the present-day British Isles during the Rhaetian (A) and Berriasian (B) stages. Maps show the position of the Aust Cliff and Westbury Garden Cliff (A) and Durlston Bay (B) localities. Note that all three assemblages are close to palaeoshorelines.

oversteps onto Carboniferous limestone at the palaeoshorelines of these islands. Westbury Formation faunas are also found in sediments filling some Carboniferous fissures, indicating transgression over exposed Carboniferous limestone karst surfaces.

The Westbury Formation consists of grey–black pyrite-rich marine shales, with thin beds of locally pyritic and/or calcitic vertebrate-rich sands, and sandy, shelly limestones. Exposures of the Westbury Formation are distinctive and easily recognisable, and many have been described in detail. In a review of 39 sections through the Westbury Formation, based on the accessible exposures at that time together with data from the literature, Sykes (1977) states that the sand and limestone bands contained within the Westbury Formation are laterally discontinuous, and cannot be used to correlate the Westbury Formation. MacQuaker (1994) stated that the Westbury Formation is composed of a stacked sequence of coarsening-upwards units, separated from one another by basal erosion surfaces, and ripple-laminated upper surfaces.

Phosphate-rich sandy units (bone beds) frequently cap the coarsening-upwards units. According to Sykes (1977), all British Rhaetic bone beds show signs of secondary deposition, i.e. all contain reworked vertebrate material. These concentrated vertebrate accumulations vary in character from exposure to exposure, however, most are thought to represent condensation deposits formed in relatively shallow water during the transgressive phases of transgressive–regressive cycles (MacQuaker, 1994). It is likely, therefore, that the bone accumulations within the Westbury Formation at separate geographical locations were formed by similar processes operating at somewhat different times; hence these accumulations cannot be associated with a single transgressive event (Storrs, 1994).

In many exposures, the basal unit of the Westbury Formation is a distinctive conglomeratic bone and pebble accumulation, resting unconformably on the eroded Blue Anchor Formation. This basal bone bed is very similar to the vertebrate-rich sand and pebble beds found capping coarsening-upwards cycles within the Westbury Formation, but it commonly has a larger average clast size.

The best-known British Rhaetian bone bed is the Aust Cliff bone bed. It is found at the base of the Westbury Formation, resting unconformably on the Blue Anchor Formation. The basal

bone bed at Aust Cliff contains a number of sedimentary features that are either distinct from other bone accumulations within the Westbury Formation, or are very exaggerated. Descriptions of the sedimentary features of the Aust Cliff basal bone bed are provided by Trueman and Benton (1997), Swift and Martill (1999), and Benton et al. (2002).

The main bone accumulation at Westbury Garden Cliff is very different in character from the basal bone bed at Aust Cliff, and contains abundant low-energy ripple and channel features, extensive phosphatisation and pyritisation. Bones are commonly preserved in small channels less than 5 cm in width, and often show preferred alignment of long axes. These features are consistent with the MacQuaker (1994) model of bone bed formation as a shallow water concentration deposit developed during periods of very low sediment supply.

1.3. The Durlston Formation

The Late Jurassic succession in southern England is characterised by a complex series of regressive shallow marine–hypersaline freshwater cycles, formed in a carbonate coastal lagoon. Capping this unit is the Late Jurassic–lowest Cretaceous Purbeck Group, exposed on the Dorset coast between Durlston Head and Swanage.

The Purbeck Group was divided into Lower, Middle and Upper parts, and all included in the Jurassic until Casey (1963) proposed to draw the Jurassic–Cretaceous boundary at the 'Cinder Bed' (bed 111 of Clements, 1993), in the Middle part of the sequence. Thus divided, the Purbeck Group is separated into the Jurassic Lulworth Formation, and the Cretaceous Durlston Formation.

The Lulworth Formation is characterised by hypersaline freshwater cycles, with common evaporites. The environment of deposition is considered to be a low-energy hypersaline lagoon, with evaporite deposition. At the top of the Lulworth beds is a conspicuous bed known as the Cinder Bed. This marks the start of the Durlston Formation, and represents a clear, regional transgression. The overlying Intermarine beds consist of a sequence of marine, brackish and freshwater limestones, interbedded with marly shales. Abundant dinosaur trackways have been recovered in this area (Wright, 1996), indicating temporary exposure of the substrate, possibly as a result of tidal cycles.

The lowest member of the Durlston Formation is the 'Broken Shell Limestone'. This bed (bed 220 of Clements, 1993) is a 2.8-m-thick sandy limestone with abundant shell fragments, and very common fragmented turtle, fish and reptile debris. The Broken Shell Limestone represents very shallow marine–coastal freshwater conditions within the Purbeck lagoon. Detrital material appears to have been derived from a large river or rivers draining land areas to the west and northwest, although the restricted sand content of the Purbeck beds suggests that the majority of the clastic debris was intraformational or derived from offshore storms. Therefore the concentration of vertebrate debris in the Broken Shell Limestone is probably due to a combination of low sedimentation rates and input from winnowed extraformational material transported into the basin during storm events.

All identifiable bone remains from the Broken Shell Member analysed in this study are fragmented remains of carapace and limb bones. Turtle carapace bones are the most abundant, all showing diploe histological structure.

2. Materials and methods

2.1. Histological nature

Buried bone contains metabolisable collagen and is a rich source of biologically limiting phosphorus. As a result the principle agent behind the initial degradation of bone is microbial attack. Microbes (bacteria, fungi and protozoans) demineralise the bone, producing one of several types of histological destruction (either tunnels or borings). These microscopic destructive features are easily recognised in thin sections or on polished surfaces of bone, and have received considerable study (e.g. Roux, 1887; Hackett, 1981; Hedges et al., 1995; Trueman and Martill, 2002).

Fossil bones used for this study were prepared

for histological examination in two ways. Petrological thin sections were obtained from some bones, whereas other bones were placed in plastic moulds and set in Epo-Kwik epoxy resin. After setting, moulds were sectioned, and polished to 1 μm grade. This method is faster and cheaper than traditional thin section preparation and polished stubs may subsequently be used for scanning electron microscopy and electron probe microanalysis (EPMA). The histological nature of fossil bones was assessed on polished thick sections and thin sections. Thick sections were examined under reflected light, and thin sections were examined under reflected and transmitted light. All bones were scored according to the Oxford Histological Index (OHI) of Hedges et al. (1995).

Most thin sections from the Rhaetic bone beds were analysed using specimens taken from the collections of the National Museum and Gallery of Wales, Cardiff. The majority of these bones came from the basal Westbury Formation bone bed at Penarth, South Glamorgan, and not from Aust Cliff or Westbury Garden Cliff. The basal bone bed at Penarth is similar taphonomically and sedimentalogically to the basal bed at Aust. A small number of thin sections and polished thick sections of bones from the Aust Cliff deposit were available, and no significant differences were seen in thin sections from Aust and Penarth, other than more extensive late diagenetic cracking and calcite veining in bones from the Aust Cliff deposit.

2.2. Mineralogy

Fresh bone crystals are non-stoichiometric apatites that most closely approximate the mineral, dahllite, a carbonated hydroxy apatite. Bone crystals are relatively unstable due to their non-stoichiometry and small size. Most fossil bones, however, are composed of francolite (carbonate fluoroapatite) and are relatively stable. The diagenetic increase in trace element content commonly seen in fossil bone is probably associated with this mineralogical change. Hence, it is important to characterise the mineralogy of fossil bone. This is easily achieved by X-ray diffraction (XRD). EPMA was also performed on a small number of samples to complement XRD analyses.

2.3. Sampling methodology

The Aust Cliff, Westbury Garden Cliff, and Durlston Bay assemblages are concentrated in single beds. In the Aust Cliff and Westbury Garden Cliff localities, the bone bed is not accessible in situ, and material was collected from fresh, unweathered, fallen blocks of bone bed found on the foreshore. The Broken Shell Member at Durlston Bay is easily accessible on the foreshore, and numerous samples were collected from the outcrop. Most vertebrate material was mechanically separated from the sediment with an engraver's drill; however, some blocks of bone bed from Aust Cliff were also digested with 5% acetic acid to liberate vertebrate debris. This treatment was tested and found to have no effect on subsequent analyses.

2.4. Preparation for analyses

For inductively coupled plasma mass spectrometry (ICP-MS) and XRD analyses, any adhering sediment was removed mechanically with an engraver's drill, together with the outer 5 mm of weathered bone surfaces, and the bone sample was then washed with distilled water, and placed in an ultrasonic tank to remove any further adhering sediment. Bones were then ground to powder with a pestle and mortar, and placed in clean glass sample vessels. Prior to further sample preparation, all sample powders were heated to 100°C for 24 h to remove any remaining water.

2.5. XRD preparation

Dried powders of bone and sediment were mounted on glass discs by mobilisation with acetone, followed by evaporation of the acetone.

2.6. ICP-MS preparation

Dried powders of bone and sediment samples (0.2 g) were digested in a Teflon beaker with HNO_3. This was heated to 200°C on a hot plate

until the sample became a nearly dry cake. After cooling, the cake was dissolved with ~15 ml of 5% HNO_3 on a hot plate, and then made up to 100 ml with 1% HNO_3 in a volumetric flask, and stored in a clean plastic bottle until required for analysis.

2.7. Sample analysis: XRD analysis

XRD spectra were obtained on a Philips PW1800 diffractometer at Bristol University. Spectra were obtained with a copper anode, operating at 45 kV and 40 mA. Full spectra were measured from 6° to 70°, with a step size of 0.02°, and step time of 2 s per step. Spectra for carbonate measurements were obtained by scanning from 51° to 53.4°, with a step size of 0.005°, and a step time of 2.5 s per step, allowing calculation of the CO_3 content of francolite to within ± 0.61 wt% (Shuffert et al., 1990).

2.8. EPMA analysis

Bones were analysed for Ca, P and F contents by wave-dispersive electron microprobe methods. The analyses were carried out at Bristol University, using a JEOL-8600 Superprobe coupled with a Link computer. Operating conditions were: accelerating voltage 15 kV, beam current 15 mA and counting times 15 s on peak, 8 s on background. Natural mineral and synthetic compounds were used as standards.

2.9. REE analysis

REE measurements were performed on a VG Plasma Quad 2+ mass spectrometer at Bristol University. The ICP-MS operated in scanning mode between masses 100.9 and 189.8, using the pulse counter, and the following isotopes were measured: ^{102}Ru, ^{139}La, ^{140}Ce, ^{141}Pr, ^{146}Nd, ^{147}Sm, ^{153}Eu, ^{155}Gd, ^{159}Tb, ^{162}Dy, ^{165}Ho, ^{166}Er, ^{169}Tm, ^{174}Yb, ^{175}Lu and ^{187}Re. Rhenium and ruthenium were used as internal standards and were kept at a constant concentration of 100 ppb for all samples and standards. Calibration was carried out using REE standards at concentrations of 0, 20, 60 and 100 ppb. All samples were run in triplicate, and at least three international rock standards and blank samples were analysed during the course of each sample interval to monitor accuracy and precision. Estimated errors (2σ) are below ± 10% in all cases.

3. Results

3.1. Histology and bioerosion

3.1.1. Westbury Formation bone beds

In total, 53 samples were scored for histology index values, and only five samples showed clear traces of microscopic bioerosion. However, all bones are recrystallised and cracked, and this diagenetic alteration may have obscured traces of internal bioerosion. All bones show evidence of diagenetic calcite and pyrite within vascular spaces, pyrite usually preceding calcite.

3.1.2. Durlston Formation bone beds

Eleven bone samples from Durlston Bay were scored for OHI values, and of these, eight bones show clear traces of bioerosion. Where present, bioerosion is relatively advanced, locally obscuring any traces of original histology.

Areas with little evidence of bone destruction, and hence high histology index values, are concentrated in the dense, cortical regions of bones from Durlston Bay. In these areas, lamellar structures may be preserved, however, diagenetic apatite recrystallisation is common resulting highly translucent bones, with a consequent loss of histological detail (e.g. Pfretzschner, 2000).

Evidence of bioerosion is common in some bones (Fig. 2), and two main types of bioerosion are found.

(1) Relatively large, branching networks of tunnels penetrating into the bone cortex from external surfaces (Fig. 2A). These tunnel systems are usually > 20 μm in diameter, and commonly infilled with pyrite. These tunnels are most likely Wedl tunnels (Hackett, 1981), and probably reflect fungal colonisation of bone surfaces.

(2) Discrete patches of dense cortical or cancellous bone showing extensive dissolution and replacement of bone (Fig. 2B) This form of destruc-

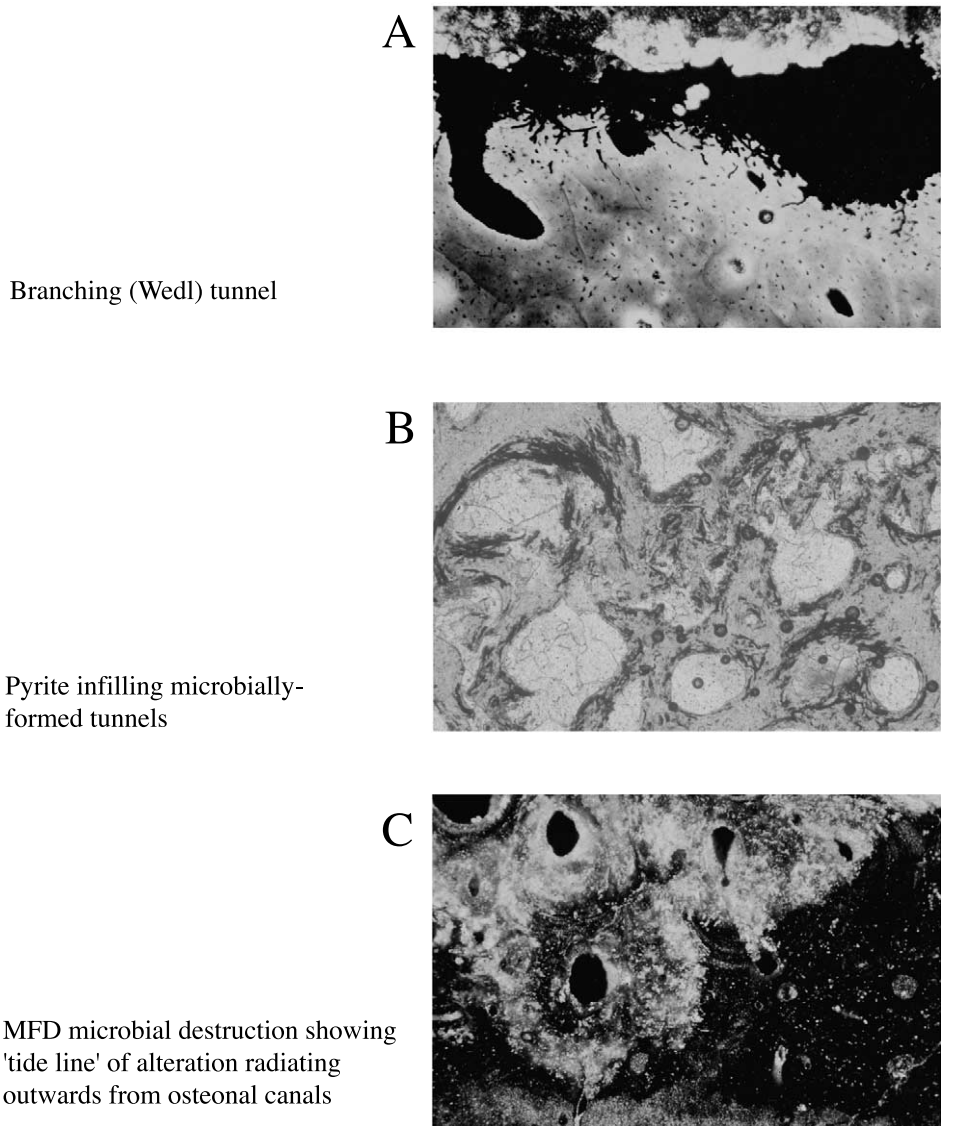

Fig. 2. Photomicrographs of turtle bone apatite from Durlston Bay showing histological damage caused by microbial activity. (A) Thin section image showing extensive Wedl-type histological alteration. Histological destruction is widespread and disseminated throughout the bone. MFD tunnels are infilled with black pyrite. Field of view = 2 cm. (B) Reflected light image showing permineralised tunnels (dark) within original bone apatite (light). Note that tunnels follow original bone structures. Field of view = 2 cm. (C) Reflected light image showing a 'tide line' of destruction concentrated around single osteons. MFD tunnels infilled with amorphous, intergrown calcite and apatite. Field of view = 1.4 cm.

tive remodelling is dispersed throughout individual bones, and may occur as permineralised tunnels, very similar to the destructive foci of Bell et al. (1996). Microprobe analyses show these tunnels to be infilled either by pyrite or calcite–apatite mineral intergrowths, but these material are amorphous or very poorly crystalline, and are difficult to characterise fully.

Histological destruction is unevenly distributed in individual bones, but appears to be initially

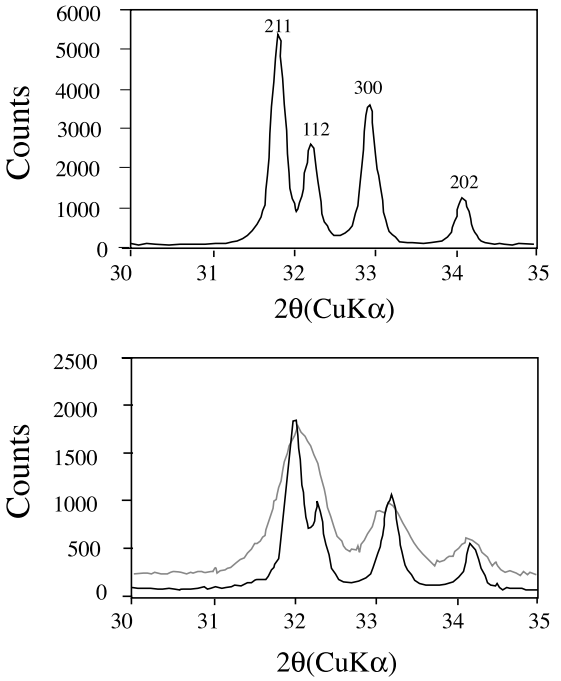

Fig. 3. XRD patterns for bone apatite. (Top) The XRD pattern of sintered bone apatite. Numbers refer to crystal reflection faces. (Bottom) XRD pattern of bone from Durlston Bay before (upper trace) and after (lower trace) heating at 800°C for 24 h. Note that after heating the XRD trace sharpens, and the broad peak between 31 and 32.5°2θ is resolved into two separate peaks.

associated with larger vascular canals, spreading out from these canals into previous unaffected bone (Fig. 2C).

3.2. XRD identification of the mineral phase

The XRD patterns of all samples show principal apatite and calcite mineral phases. The apatite phase is difficult to assess, as the 112 peak is very poorly developed, and frequently masked by the broad 211 peak (Fig. 3). The peak intensity order recovered from fossil bone apatite is as follows: (211, 112), 300, 202. This may be compared with the peak order recorded for unweathered francolites: (121, 211), 112, 300, 202 (Jarvis, 1992). The broad, poorly defined 211 peak probably masks the relatively weak 112 peak, producing higher than expected intensities for the 112 reflection. This effect is clearly seen when fossil bone samples are heated over 800°C in platinum crucibles. Recrystallisation occurs in the sample, producing sharper peaks (e.g. Person et al., 1996), and allowing identification of the 112 peak. Some loss of carbonate from the apatite lattice also occurs, reducing the relative size of the 211 peak, producing an XRD trace similar to that of sintered biological bone (Fig. 3).

3.3. Crystallinity values

Crystallinity index values for bones from Aust Cliff and Durlston Bay were determined according to the method of Person et al. (1996), in which fresh bone has a crystallinity index of less than 0.1. A wide variation in crystallinity index values

Table 1
Crystallinity of bone apatite samples from the Aust Cliff and Durlston Bay localities

Sample	Crystallinity	Sample	Crystallinity
Aust Cliff		Durlston Bay	
A1	0.59	S1	0.57
A2	0.60	S3	0.42
A3	0.73	S4	0.43
A4	0.56	S5	0.45
A5	0.76	S6	0.48
A7	0.48	S7	0.40
A9	0.61	S9	0.44
A10	0.74	S10	0.34
A11	0.55	S11	0.42
A12	0.53	S20	0.35
AS1	0.60	S21	0.46
AS2	0.60	S22	0.40
AS3	0.61	S23	0.36
AS4	0.65	S24	0.46
AS5	0.64	S25	0.39
AS6	0.60	S26	0.40
AS7	0.63	S27	0.50
AS8	0.72	S29	0.40
AS9	0.64	S30	0.38
AS11	0.53	S31	0.34
AS12	0.86	S33	0.43
		S35	0.37
		S36	0.37
		S37	0.39
		S39	0.55
Mean	0.632		0.421
S.D.	0.09		0.05

Crystallinty was determined from XRD patterns following the method of Person et al. (1996).

is seen in both sample sets (Table 1). The crystallinity index values are distributed normally in both assemblages, with significantly higher mean crystallinity in the bones from Aust Cliff than in those from Durlston Bay (mean crystallinity of Aust samples = 0.632, S.D. = 0.09, mean crystallinity of Durlston Bay samples = 0.421, S.D. = 0.05). A Student's *t*-test shows that the means are significantly different at the 1% probability level. XRD patterns were also used in an attempt to measure apatite structural carbonate contents following the peak-pair splitting method of Shuffert et al. (1990). However, this method was found to be unreliable with the samples and equipment used, as repeated analyses yielded inconsistent results (> 50% error in some cases).

3.4. Ca/P ratios

Ca/P values were determined in individual samples by EPMA. The mean Ca/P ratio from Durlston Bay turtle apatite is 2.34 ($n = 12$, S.D. = 0.03). From the Aust Cliff sample, shark tooth dentine gives an average Ca/P ratio of 2.34 ($n = 22$, S.D. = 0.04) and 2.45 ($n = 15$, S.D. = 0.03) and bone gives 2.48 ($n = 15$, S.D. = 0.02). Assuming an ideal formula of $Ca_{10}(PO_4,CO_3)_6OH_2$, this corresponds to structural carbonate contents of 2.97 wt% for bone from Durlston Bay and 4.91 wt% for bone from Aust Cliff. These values are generally lower than the inconsistent values determined by the peak-pair spacing method, and emphasise the difficulty of using the peak-pair method on fossil bone samples.

3.5. Fluorine content

Fluorine concentrations were measured directly in selected bone samples by EPMA. Fluorine concentrations were determined by multiple analyses in individual bone samples. The measured fluorine concentrations in fossil bones are uniformly higher than biological bone apatite, and typical of the 'excess fluorine' (F content > 3.77 wt%) apatites of McClellan and Van Kauwenbergh (1990). This result confirms that the mineralogy of the fossil bone apatite is principally francolite, similar to sedimentary apatites (e.g. Jarvis, 1992). Although F levels vary, individual bones from Aust Cliff apparently have higher F contents (3.95 wt%, $n = 4$) than bones from Durlston Bay (3.65 wt%, $n = 3$), although the significance of this result is uncertain as the sample numbers are low.

3.6. REE contents of marine bones

The REE concentrations in bones from Aust Cliff and Durlston Bay are listed in Table 2. The total REE values of bones from the Aust assemblage vary from 5400 ppm to < 100 ppm, and from the Durlston Bay assemblage, from 6900 ppm to < 100 ppm. This large variation in total REE may be due in part to variation in apatite/calcite ratios in the bone samples, but the relationship is complicated by the influence of the bone structure on the rate and degree of REE incorporation. The REE may be fractionated within bones, particularly within dense cortical bone (Williams and Potts, 1988; Trueman and Tuross, 2002), and this effect could potentially lead to increased geochemical variation that does not reflect mixing. This effect can be minimised by sampling equivalent small bone fragments in all assemblages under study, after removal of the outer 5 mm of bone.

The average total REE concentration in these bones is 2250 ppm (S.D. = 1500). This concentration is similar to REE concentrations in bones from coastal marine and terrestrial sediments (Trueman and Benton, 1997; Trueman, 1999), and slightly higher than REE concentrations in ichthyoliths, which generally contain c. 1000 ppm total REE (e.g. Grandjean et al., 1987; Grandjean-Lécuyer et al., 1993; Wright et al., 1984; Bertram et al., 1992). However, all fossil bones contain considerably higher concentrations of REE than phosphorite deposits (Altschuler, 1980), and modern shelf and deep-sea sediments (Elderfield and Pagett, 1986).

4. Discussion

4.1. Bioerosion and survival of bone

Bioerosion is commonly seen as incompatible

Table 2
REE concentrations (ppm) in bones from Aust, Westbury Garden Cliff, and Durlston Bay

		La	Ce	Pr	Nd	Sm	Eu	Gd	Tb	Dy	Ho	Er	Tm	Yb	Lu	Total REE
Aust																
Cp (P,l)	A1	839	2220	309.9	1266	242.5	35.83	205.4	30.6	140.8	23.56	49.25	4.11	18.63	2.32	5392
Trab (I)	A2	522.8	734.2	86.74	307.3	46.29	8.74	55.65	7.87	40.85	8.13	18.48	1.6	7.31	0.89	1847
Trab (P)	A3	504.1	897.8	118.6	465.8	82.08	13.77	75.22	11.36	56.3	10.38	23.37	2.26	10.86	1.31	2273
Cp+Cl (P,l)	A4	803.4	1633	193.4	743.7	131.5	23.35	135.1	20.03	102.2	19.07	40.67	3.51	16.82	2.09	3868
Cp+Cl (P,v)	A5	502	1250	191.7	822	160.8	24.99	125	18.16	84.45	13.42	29.37	2.39	10.89	1.32	3236
Fin spine (HY)	A6	470.1	609.7	74.48	270.3	40.1	7.38	46.53	7.1	39.01	8.24	19.51	1.93	9.17	1.14	1605
Trab (I)	A7	333.1	644.2	95.5	368.8	63.82	10.61	60	8.76	44.04	7.81	16.46	1.44	6.93	0.78	1662
Cp (P)	A8	400.4	1110	149	618	108	23.7	104.3	14.19	68.1	10.1	20.5	**1.57**	8.811	**1.12**	2635
Fin spine (HY)	A9	463.3	1260	174	703	135	25.5	115.4	15.82	72.5	11.1	24.2	**1.57**	9.13	**0.69**	3009
Cp (P,l)	A11	1.92	2.700	0.3	3.57	1.75	0.23	0.41	0.06	0.44	0.14	0.42	**2.10**	0.08	**1.33**	12
Trab (P,l)	A12	691	1250	134	513	79.2	18.3	95.97	13.49	70.7	13.7	30.7	**2.7**	14.9	**2.05**	2925
Cp+Cl (P,l)	A13	593.8	1138	151.8	562.6	112.2	26.27	123.6	15.02	78.77	13.43	29.63	2.67	11.52	1.74	2861
Fin spine (HY)	A14	172.8	108.8	10.4	36.39	6.57	1.36	**8.81**	0.98	7.89	**2.06**	4.88	0.66	2.72	0.37	353
Tooth (PY)	A15	1753	3096	398.9	1347	252.3	37.32	181.2	25.3	138.2	24.94	57.47	5.9	25.84	3.48	7347
Tooth (IC)	AS1	437.1	359.5	28.22	84.81	14.29	3.86	**25.56**	2.83	18.16	3.92	11.13	1.23	6.27	**2.57**	971
Trab (I)	AS2	246.6	274.0	23.94	78.54	17.01	3.34	**21.59**	2.47	13.72	2.86	7.06	0.75	4.18	**3.55**	674
Fin spine (HY)	AS3	567.1	1089	125.9	418.5	82.58	16	98.12	11.29	59.11	9.88	22.34	2.14	10.16	**3.27**	2512
Trab (IC)	AS4	314.9	565.2	57.21	178	33.8	6.47	**44.52**	4.84	25.9	4.32	9.35	0.92	4.9	**2.88**	1206
Cp+Cl (I)	AS5	581.6	1513	188.6	628.9	122.8	23.38	**140.37**	15.22	73.28	10.38	21.74	1.78	8.07	**3.4**	3189
Cp+Cl (I,l)	AS7	456	968.3	118.7	411.1	86.88	17.42	**93.06**	10.69	52.97	8.24	17.37	1.56	7.12	**2.01**	2156
Cp+Trab (I)	AS8	309.6	277.9	21.49	62.09	10.75	3.05	**19.1**	2.14	13.45	2.99	7.43	0.81	4.63	**1.78**	716
Cp+Trab (I,v)	AS9	510.8	770.4	77.26	246.1	45.35	10.27	**61.65**	6.98	38.38	6.79	15.51	1.55	7.15	**2.16**	17.36
Cp (P,l)	AS11	181	143.3	21.57	78.9	13.34	3.49	20.12	2.39	13.79	2.75	6.35	0.65	2.97	0.4	491
Westbury Garden Cliff																
Pv	W2	523.9	1200	178.9	706.9	162.8	38.7	166.9	22.56	116.8	**19.5**	40.84	3.66	16.15	1.9	3180
Indet fish (v)	W3	670.3	1463	232.7	922.8	213.6	50.97	226.4	30.24	158.3	25.5	56.16	5.43	22.82	2.92	4081
I (v)	W4	722.3	1408	244.3	1018	246.9	57.18	258.8	34.48	177.3	30.09	68.98	7.05	28.94	4.12	4307
Tooth (SU)	W5	660.5	1262	179.5	697.1	157.6	37.32	**181.23**	25.3	138.2	**24.95**	57.47	5.9	25.84	3.48	3251
Ct (I)	W6	552.8	1140	164.6	661.8	155.2	36	**175.5**	23.6	127.4	**21.3**	48.85	4.92	19.59	2.84	2938
Rib (I)	W7	693	1057	137.4	499.4	108.8	34.06	136.2	19.4	113.6	**21.18**	49.7	5.59	22.83	3.43	2880
Fin spine (HY)	W8	372.2	824.7	111.8	433.1	94.82	23.25	**109.0**	15.08	82.62	**14.34**	32.48	3.39	13.8	1.98	2009
Durlston Bay																
Turtle scute	S2	465.1	681.6	89.5	350	49.25	8.72	**47.89**	6.6	33.57	**6.95**	18.8	2.02	10.42	1.33	1717
Turtle scute	S3	226	270.5	30.48	126.1	15.86	3.25	**17.85**	2.5	13.73	**3.3**	9.51	1.14	5.82	0.84	705.7
Turtle scute	S4	160.6	220.4	28.68	118.7	19.78	3.64	**18.56**	2.67	15.4	**3.29**	8.39	0.97	5.1	0.63	585.1
Turtle scute	S5	299	379.7	44.03	174	25.22	4.37	**27.08**	3.67	20.58	**4.53**	12.85	1.47	7.97	1.12	973.9
Fish scale	S6	119.6	266	39.16	169.8	33.02	4.88	28.91	4.53	23.56	**4.33**	10.11	1.06	4.8	0.65	706
Limb bone (I)	S7	128	231.1	39.24	169.1	30.99	4.77	25.44	3.85	19.05	**3.6**	8.55	0.79	4.09	0.56	665.5
Limb bone calcite fill	S8*	22.73	43.76	6.61	28.34	6.24	8.6	4.75	0.66	3.39	**0.64**	1.61	0.12	0.75	0.1	127.7
Limb bone (I)	S9	414.9	725	77.4	303	49.2	10.5	**28.02**	7.7	42.6	**3.6**	18.7	**1.14**	8.32	**0.72**	1657

Table 2 (*Continued*).

		La	Ce	Pr	Nd	Sm	Eu	Gd	Tb	Dy	Ho	Er	Tm	Yb	Lu	Total REE
Turtle scute	S10	491.8	756	90.2	353	41.3	9.71	**56.18**	6.39	34	**6.82**	17.2	**1.91**	10.61	**1.57**	1810
Turtle scute	S11	197.5	287	34.3	15	21.4	4.03	**0.26**	2.31	12.9	**0.16**	7.73	**0.09**	4.84	**0.07**	722
Turtle scute	S20	293.9	380	41.37	169.7	26.92	4.2	26.11	2.73	14.34	3.4	8.88	1.15	4.55	4.91	982.1
Turtle scute	S21	512.7	803	87.77	358.8	50.07	7.58	56.58	6.08	32.72	7.36	16.91	2.06	7.99	2.15	1952
Turtle scute	S22	318	509.7	58.73	249.6	40.44	5.57	41.91	4.72	25.58	5.99	13.49	1.81	7.24	3.08	1286
Turtle scute	S23	590	915.5	104.6	434.4	56.77	9.57	70.05	7.32	38.8	8.57	19.35	2.4	9.48	1.5	2268
Turtle scute	S24	750.8	1974	317.6	1367	252.9	35.72	206.5	24.45	114.8	19.99	40.34	5.17	20.4	4.2	5134
Turtle scute	S25	359.9	458.6	48.91	200.6	28.23	4.49	33.85	3.69	21.76	5.36	12.89	1.68	7.06	2.61	1190
Turtle scute	S26	621.8	1099	135	585.2	88.4	13.8	102.9	11.15	6	12.81	28.04	3.29	12.16	5.28	2779
Limb	S27	470.8	942.1	114.5	477	72.41	10.9	76.01	8.51	46.19	9.6	21.05	2.61	10.65	2.53	2265
Turtle scute	S28	429.2	677.6	75.61	313.4	43.97	6.75	48.75	5.11	29.59	6.48	15.54	1.85	7.72	2.13	1664
Turtle scute	S32	355.3	840.7	111.1	471.7	83.63	11.57	73.78	8.61	41.04	8.03	16.73	2.03	8.35	3.98	2036
Limb	S33	478.4	1020	128.2	543.8	83.66	11.98	79.74	8.83	46.12	9.49	20.64	2.46	9.52	2.78	2446
Turtle scute	S34	429.4	590.9	63.02	253.8	33.65	5.43	41.93	4.34	25.7	6.4	14.26	1.93	7.88	1.71	1480
Limb	S36	977.9	2716	420.4	1858	340.6	45.52	274.5	32.49	154.2	27.61	57.38	6.96	28.03	4.14	6944
Turtle scute	S37	514.1	837.2	96.27	394.9	55.53	8.24	60.55	6.16	33.8	7.19	16.33	2.04	7.47	4.22	2044
Turtle scute	S39	760.6	1793	238.4	992.2	170.3	24.39	162.2	19.16	96.01	18.49	40.13	4.88	19.83	3.86	4344

Figures in boldface refer to measurements where ICP-MS quality control statistics fall below acceptable standards. S8* = permineralising calcite recovered from bone S7. Teeth were not included in tests of variance.

Description abbreviations. Taxonomic: I = Indeterminate vertebrate, P = *Pachystropheus rhaeticus*, PL = Indeterminate pleisiosaur, HY = *Hybodus minor*, PY = *Polyacrodus* sp., IC = Indeterminate ichthyosaur, SU = *Severnichthys* sp. Osteological/Histological: l = limb element, v = vertebra, Cp = dense compact bone, Ct = cortical bone from long bones, Cl = cancellous compact bone, Trab = trabecular bone.

with survival of bone into the fossil record, as in modern and archaeological cases bioerosion rapidly progresses to complete destruction of the bone (e.g. Hedges et al., 1995). The generally excellent histological condition of fossil bones supports this view, but bioerosion is found in a small percentage of cases (Trueman and Martill, 2002). This means that where extensive bioerosion is found in fossil bones (as in the Durlston Bay bone bed) some explanation for the survival of bone is required.

The most likely mechanism for halting bioerosion is a change in the physico-chemical nature of the bone environment. This may occur as by-products of microbial metabolism build-up within the bone, eventually exceeding microbial tolerance levels. pH is one possible inhibiting condition. If such microenvironmental conditions coincide with conditions favourable for rapid mineral growth, then the microbial tunnels may themselves be infilled, preserving a bioeroded bone. We suggest that the bones deposited within Durlston Bay initially provided a favourable environment for microbial growth, but that conditions within the bone deteriorated to such an extent that microbial metabolism could no longer operate. The new conditions were favourable for sulphate-reducing bacteria, which initiated deposition of pyrite within vascular and other pore spaces. This suggests that each bone remained a relatively closed environment, and diffusion of microbial by-products away from the bone was not sufficient to refresh the internal environment. The REE chemistry of bones from Durlston Bay provides some evidence to support the suggestion that bones may develop and maintain an internal chemistry distinct from that of their immediate surroundings.

In oxic pore waters, Eu exists as Eu^{3+}; the reduced form, Eu^{2+}, is only stable in hydrothermal systems, euxinic, and organic-rich saline marine waters (Brookins, 1988). Like the rest of the REE, Eu replaces Ca in the apatite lattice. The relative ease of forcing a replacement cation into a host cation site is largely controlled by the difference in ionic radius and charge between the replacement ion and the host ion, and the amount of strain that can be accommodated by the crystal lattice. The relatively large Eu^{2+} ion is more compatible in the apatite lattice than the smaller Eu^{3+} ion because of its divalent charge. However, apatite has a relatively low Young's modulus compared to calcite, indicating that calcite will show a greater preference for Eu^{2+} compared to the trivalent REE than will apatite. Thus, if reduced Eu^{2+} were present in the pore waters from which both authigenic apatite and calcite incorporated REE, partitioning of Eu between apatite and calcite would be expected. Such partitioning is seen very clearly in bone–calcite couples from Durlston Bay (Fig. 4), Eu^{2+} is partitioned strongly into calcite, producing a positive Eu anomaly. This leaves pore waters depleted in terms of Eu, and thus apatite acquires a negative Eu anomaly.

Eu^{2+} partitioning between apatite and calcite suggests that the conditions during permineralisation must have overlapped both the Eu^{2+} and the $CaCO_3$ stability fields. This allows the Eh–pH conditions experienced during this period of diagenesis of the bone material to be constrained (Fig. 5). The predicted Eh–pH field for the growth of calcite and stability of Eu^{2+} lies within the field of organic-rich saline waters (Garrells and Christ, 1965). In contrast, the sediment matrix from Durlston Bay shows a negative Ce anomaly, and no Eu anomaly. This reflects the sedimentological data suggesting that the Durlston Bay environment was relatively oxic. The sedimentology of the Durlston Bay assemblage also suggests that it was deposited in an oxic, low-organic-content environment.

Hence, the presence of Eu anomalies *within* bones implies locally reducing conditions, most likely caused by the microbial decomposition of organic matter (Rae and Ivanovitch, 1984; Hubert et al., 1996). The REE patterns of apatite and calcite therefore show that the environment inside the bone became chemically distinct from that outside the bone. The preservation of heavily bioeroded bones at Durlston Bay can be explained if the implied internal chemical environment (anoxic, low pH) inhibited collagen-metabolising microbes, but was favourable for sulphate reducers.

Destructive microbial remodelling of bones from Durlston Bay is represented in the range of preservation states observed in the available

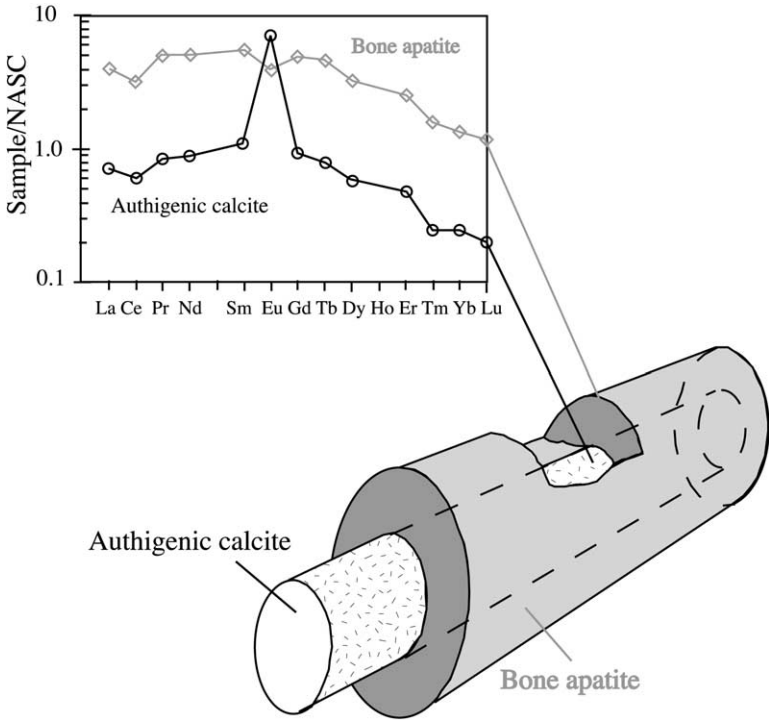

Fig. 4. Diagram showing the REE pattern developed in coexisting bone apatite and perminearlising calcite from an unidentified bone fragment from Durlston Bay (S7). Note the large positive Eu anomaly in the calcite and the corresponding negative Eu anomaly in the bone apatite, suggesting partitioning under closed conditions.

sample and appears to have proceeded in a systematic fashion:

- The vascular network of the bone was completely saturated by pore waters. This is clearly seen where precipitation of pyrite has occurred within these vascular canals with no dissolution of the surrounding apatite. In this case, the morphology of the vascular network, including the osteocyte lacunae, and lacunar processes are very well preserved.
- Microbial metabolism of bone collagen caused dissolution of apatite and the growth of invasive networks of tunnels. These tunnels spread via the vascular network, and increased the total porosity and permeability of the bone.
- Continued dissolution of apatite throughout the whole of the vascular network of the bone resulted (in some cases) in the localised loss of 80–90% of the original bone apatite, and almost total loss of any histological features.
- pH levels fell in localised regions of bone, possibly as a result of microbial activity. Low-pH and low-Eh conditions were maintained within the bone, distinct from those outside of the bone. This fall in pH and Eh inhibited further microbial dissolution of bone, and encouraged rapid precipitation of diagenetic minerals such as pyrite, preserving the bioeroded bone. During this time Eu was reduced and partitioned between authigenic apatite and calcite. The extent of pyrite permineralisation and destructive remodelling appears to be controlled in part by the ease of passage of pore waters through the bone. Thus 'tide lines' of displacive permineralisation are seen at the boundaries between cortical and trabecular bone, and around osteonal canals (Fig. 2C).

All these observations suggest that chemical exchange between the internal and external bone environments was limited, and that the bone experienced closed conditions during early diagenesis.

All bone samples analysed in this study are

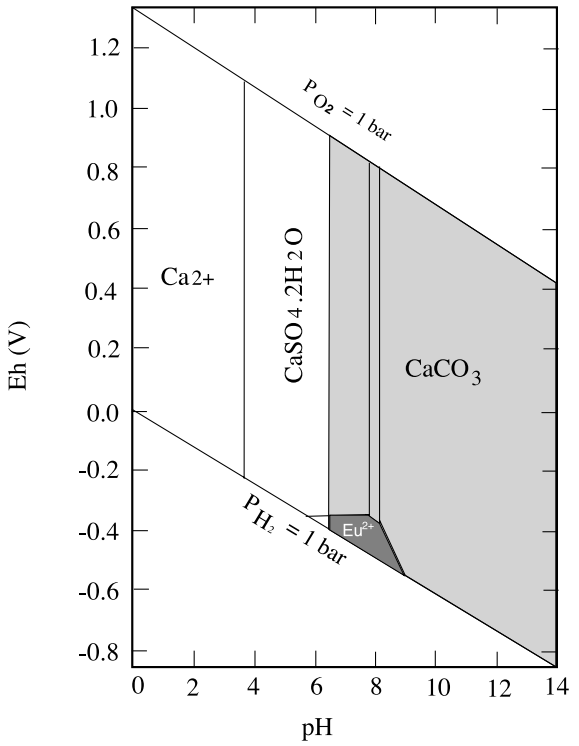

Fig. 5. Eh–pH diagram for part of the systems Eu–C–OH and Ca–C–OH–S. Dark-shaded areas are the fields of Eu^{2+} stability and $CaCO^3$ stability. After Brookins, 1988.

composed primarily of carbonate–fluorapatite (francolite). The fluorine and carbonate contents indicated by EPMA analyses are consistent with other sedimentary apatites and other records of fossil bone francolite (e.g. Hubert et al., 1996). However, XRD patterns suggest that the mineralogy of this francolite varies both within and between assemblages. The large errors associated with XRD analyses encountered during this study meant that no further implications could be drawn from variations in apatite mineralogy. Such variations may also yield information concerning the recrystallisation process, and merit further investigation with state-of-the-art equipment.

4.2. Geochemical taphonomy

The controls affecting the final trace element composition of any exposed bone may be expressed as:

$$X_{i(\text{bone final})} = f(X_{i(\text{bone initial})},\ X_{i(\text{pore water})},\ D,\ K,\ H,\ M,\ T) \quad (1)$$

where X_i is the concentration of trace element (i) in system X, D is the apatite–fluid partition or adsorption coefficient, K is the chemistry of the microenvironment of burial, H is the hydrology of the microenvironment, M is the bone microstructure and T is the length of exposure (Trueman, 1999).

While the trace element content of individual bones may be related to the pore water chemistry in the early burial environment, the *variation* in REE concentrations of equivalent bones within an assemblage is controlled by sedimentologic and taphonomic variables:

$$V_{(\text{as})} = f(V_{(\text{b.e.})},\ R_{(\text{d})}) \quad (2)$$

where $V_{(\text{as})}$ is the variation in trace element content of bones within an assemblage, $V_{(\text{b.e.})}$ is the variation on the original geochemical environments experienced by the bones that are incorporated into the final deposit, and $R_{(\text{d})}$ is the rate of introduction of bones into the final assemblage.

This suggests that bones from assemblages with rapid rates of accumulation (i.e. low time averaging) should display relatively homogeneous trace element concentrations, as the bones will be concentrated rapidly in similar depositional environments. Assemblages with similar accumulation rates should show greater variation in trace element patterns if the source area for the bones is a more complex, varied environment with different relative proportions of trace elements in the different subenvironments (Fig. 6).

Ideally, geochemical techniques could be tested by assessing trace element variation in a series of marine vertebrate assemblages with known absolute rates of formation. It is difficult to establish absolute rates of formation in any environment, especially over the relatively short time spans likely involved in trace element uptake by bones. However, it is possible to set up an equivalent test

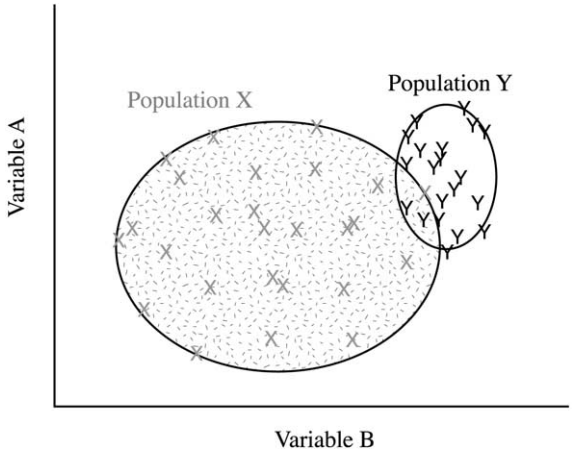

Fig. 6. Relationship between sample variance and mixing. The diagram represents the distribution of values of variables for two populations of fossils. Variables *A* and *B* may be any character of a fossil, providing that the character is developed during early diagenesis (e.g. trace element content, composition of organics, surface morphology). In this case, sample X has a wider range in values for variables *A* and *B* than sample Y (tested statistically by a one-tailed *F*-test). This implies that sample X is taken from a mixed (time and/or space-averaged) assemblage, and sample Y from a relatively unmixed, 'snapshot' assemblage. The test assumes that the processes responsible for the development of variables *A* and *B* were equally varied during the formation of the two assemblages. Note that samples may or may not be distinct in terms of variables *A* and *B*.

by manipulating existing data bases. A series of papers describe REE variation in conodonts from the Devonian Coumiac limestone of southern France. Girard and Albarède (1996) provide an extensive data set of REE contents in 78 individual conodonts from two quarries. Pooling all the conodonts from each quarry provides two analytically averaged assemblages spanning from the late *rhenana* to middle *triangularis* zones (from Girard and Albarède, 1996). Grandjean-Lécuyer et al. (1993) also present REE contents of conodonts from the Coumiac limestone, but in this study, REE data are presented from individual conodont elements within single assemblage populations. These population samples represent relatively unmixed, low-time-averaged assemblages.

Thus, if geochemical techniques are successful they should be able to distinguish between these two types of sample on the basis of trace element variation: the analytically averaged samples should show significantly more variation than the single assemblage samples. Comparison of variation is performed as an *F*-test on log-transformed ratios of shale-normalised REE values. This assumes that the range of early depositional environments available during formation of the assemblages under investigation was similar.

By pooling the data from Girard and Albarède (1996) and Grandjean-Lécuyer et al. (1993) we can produce three artificially averaged assemblages (two from Girard and Albarède, 1996; one by summing all data from Grandjean-Lécuyer et al., 1993). Splitting the data provided by Grandjean-Lécuyer et al. (1993) gives us a comparable set of unaveraged populations.

Eq. 2 predicts that the artificially averaged assemblages should show significantly greater variation in terms of REE contents than individual populations from the same locality. This predic-

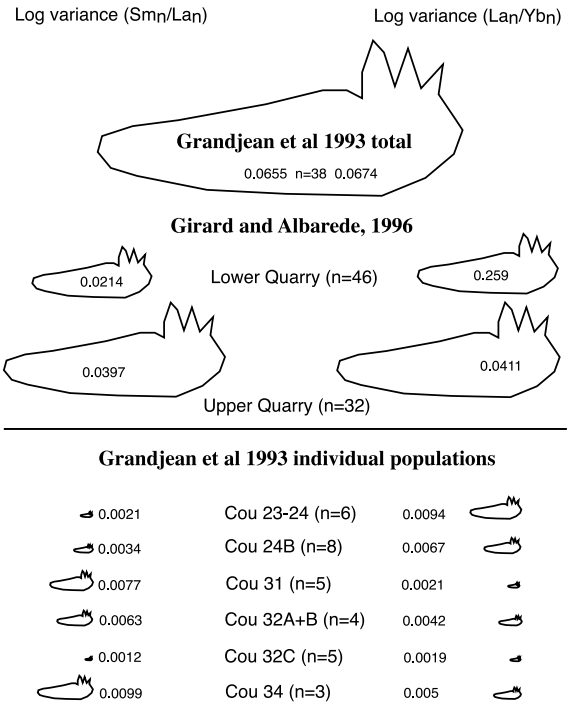

Fig. 7. Log-transformed variances of populations of conodont elements taken from Grandjean-Lécuyer et al. (1993) and Girard and Albarède (1996). Despite small sample numbers for individual assemblage populations, their variances are still significantly different (*F*-test) from all pooled (analytically averaged) samples.

Table 3
Variance in REE ratios in Devonian conodonts from the Coumiac Limestone

	Variance	*n*
Girard and Albarède (1996) pooled samples		
(Sm/La)n (LOG)	0.0294	78
(Sm/Yb)n (LOG)	0.0156	78
(La/Yb)n (LOG)	0.0328	78
Lower Quarry		
(Sm/La)n (LOG)	0.0214	46
(Sm/Yb)n (LOG)	0.0184	46
(La/Yb)n (LOG)	0.0259	46
Upper Quarry		
(Sm/La)n (LOG)	0.0397	32
(Sm/Yb)n (LOG)	0.0119	32
(La/Yb)n (LOG)	0.0411	32
Grandjean-Lécuyer et al. (1993) pooled samples		
(Sm/La)n (LOG)	0.0655	38
(Sm/Yb)n (LOG)	0.0064	38
(La/Yb)n (LOG)	0.0674	38
Cou 23-24		
(Sm/La)n (LOG)	0.0021	6
(Sm/Yb)n (LOG)	0.00601	6
(La/Yb)n (LOG)	0.00943	6
Cou 24B		
(Sm/La)n (LOG)	0.0034	8
(Sm/Yb)n (LOG)	0.0065	8
(La/Yb)n (LOG)	0.0067	8
Cou 31G		
(Sm/La)n (LOG)	0.0077	5
(Sm/Yb)n (LOG)	0.0028	5
(La/Yb)n (LOG)	0.0021	5
Grandjean-Lécuyer et al. (1993) split samples		
Cou 32A+B		
(Sm/La)n (LOG)	0.0063	4
(Sm/Yb)n (LOG)	0.0167	4
(La/Yb)n (LOG)	0.0042	4
Cou 32C		
(Sm/La)n (LOG)	0.0012	5
(Sm/Yb)n (LOG)	0.002	5
(La/Yb)n (LOG)	0.0019	5
Cou 34		
(Sm/La)n (LOG)	0.0099	3
(Sm/Yb)n (LOG)	0.003	3
(La/Yb)n (LOG)	0.005	3

Data from Girard and Albarède (1996) and Grandjean-Lécuyer et al. (1993). 'Pooled' variance is the variance in an analytically averaged sample composed of all conodonts measured in the Coumiac Quarry sequence with no stratigraphic control. Split samples represent samples with lower analytical averaging. Split samples from the Grandjean-Lécuyer et al. (1993) assemblage are multiple samples of different individual conodont elements from single depositional horizons. Despite low sample numbers, all pooled samples are significantly more varied in terms of their REE composition than all split samples (*F*-test 0.05% level).

tion may be easily tested (Fig. 7). Despite very low sample numbers, the population samples from the data set of Grandjean-Lécuyer et al. (1993) are still significantly less varied (*F*-test, 0.01 level) than the analytically averaged samples of either Girard and Albarède (1996), or the pooled sample of Grandjean-Lécuyer et al. (1993).

This shows that REE data can discriminate between high- and low-averaged samples from marine settings. We apply the same method to the Aust, Westbury and Durlston formations (Table 3). Note that the Aust assemblage is significantly more varied than both the Westbury and Durlston assemblages, and that the Westbury and Durlston assemblages are statistically similar in terms of trace element variation (Table 4).

The results above suggest that the Aust assemblage is more mixed (more time and/or space averaged) than either the Westbury or Durlston assemblage. This conclusion agrees with what would be expected given the sedimentological and taphonomic characteristics of the deposits. The bone bed at Aust Cliff contains abundant terrestrial and marine remains, including dinosaur, icthyosaur and plesiosaur remains, together with reworked Carboniferous shark teeth, common chondrichtyian, dipnoan and saurichthyian fishes; and choristoderid reptiles. The deposit itself contains abundant evidence for high-energy deposition, such as a pronounced erosive base, reverse and normal grading in a matrix-supported conglomerate, and large (>10 cm diameter) rip-

Table 4
Significance level of difference in variance between two assemblages

	Pr/Yb	Sm/La	Sm/Yb	La/Yb	$Ce_{(anom)}$
A vs W	0.01	0.01	0.01	0.01	0.01
A vs D	0.01	0.05	0.01	n.sig	0.01
W vs D	n.sig	n.sig	n.sig	0.01	n.sig
A+W vs D	0.01	0.05	0.05	0.05	0.01

A = Aust Cliff, W = Westbury Garden Cliff, D = Durlston Bay, $Ce_{(anom)}$ = cerium anomaly as defined by Elderfield and Greaves, 1982. All significance tests were performed on log-transformed ratios of shale-normalised REE values. Note that the Aust assemblage is significantly more varied than both the Westbury and Durlston assemblages, and that the Westbury and Durlston assemblages are statistically similar in terms of trace element variation.

up clasts. By contrast, the approximately contemporaneous Westbury Garden Cliff deposit contains a relatively restricted fauna, dominated by the choristodere *Pachystropheus* and small fish remains. The deposit is a thin sandy conglomerate, with abundant evidence to suggest that the Aust Cliff deposit is not taphonomically equivalent to the Westbury Garden Cliff assemblage. Given that all sampled bones were broadly equivalent in terms of microstructure (or at least equally varied), the higher diversity recorded from the Aust Cliff bone bed results from taphonomic reworking and enrichment and does not reflect local differences in diversity within the Westbury Basin. The Aust Cliff assemblage represents a time-averaged sample recording regional (multi-habitat) diversity, whereas the Westbury Garden Cliff assemblage is more of a 'snapshot'-type assemblage recording restricted local diversity (closer to within-habitat diversity). However, the REE data also indicate that the Upper Triassic Westbury Garden Cliff and Lower Cretaceous Durlston Bay assemblages are comparable in terms of the extent of mixing. This information could not be obtained from traditional taphonomic analysis. The geochemical taphonomic equivalence of these two assemblages can be used as evidence for isotaphonomy, allowing comparisons of diversity differences that are likely to reflect true ecological differences (Behrensmeyer and Hook, 1992). However, Eq. 2 states that the geochemical variation of two assemblages may be used to infer relative mixing only if one makes the assumption that the two assemblages formed from an equivalent initial range of depositional environments. As this assumption is difficult to justify beyond broad sedimentological observations, it is probably safer to restrict comparisons of geochemical variation to within-basin studies. We cannot compare the results from Aust, Westbury and Durlston assemblages to those from the Coumiac limestone and other marine localities, as the marine assemblages consist mainly of teeth and conodont elements, and as such may be inherently less varied than bones. Furthermore, the range of early depositional environments that could have contributed bones to the coastal assemblages used in this study would have been greater than environments available during the formation of open marine assemblages.

5. Conclusions

Combined geochemical, mineralogical and histological studies can yield considerable information regarding the conditions of deposition and diagenesis experienced by bones in marine settings. In one example (Durlston Bay) it is possible to constrain the chemistry of the environment of diagenesis with relative precision, and to show that the chemical environment inside the bone was distinct (low pH, reducing) from that of the surrounding sediment. Furthermore, this distinct chemical environment was maintained for sufficient amounts of time to fractionate trace elements between diagenetic permineralising minerals. The cause of this distinct chemical environment is likely to have been microbial metabolism of collagen. Many bones from Durlston Bay preserve traces of this microbial activity (bioerosion), which was initiated in relatively fresh bones. Bioerosion is relatively rare in fossil bones, presumably because it leads to increased porosity and permeability, increased pore water flow through the bone, and accelerates dissolution of bone apatite (Trueman and Martill, 2002). In the case of the Durlston Bay material, bones have survived into the fossil record because low-pH and low-Eh conditions were maintained within the bone. These conditions inhibited further microbial activity, and enhanced rapid pyrite mineralisation. Experiments investigating the mineralisation of soft tissue demonstrate that closed, mildly acidic conditions are favoured by rapid apatite mineralisation (Briggs and Kear, 1994). Thus, conditions within the bone may also encourage growth of authigenic apatite, and hence enhance preservation potential.

The process of fossilisation of bone is therefore shown to be a complex interaction of microbial activity, hydrology and local chemistry. Furthermore, the chemistry of the surrounding sediment may be a poor indication of the chemical conditions that prevailed during bone diagenesis and vica versa. This may have profound implications

as it follows that the geochemistry of fossil bone, particularly the redox chemistry, may provide a poor record of the environment of deposition, and thus great care should be taken when interpreting environmental conditions from the chemistry of fossil bone apatite. For instance, the Durlston Formation clearly represents oxic carbonate sedimentation within saline waters with relatively low organic content; however, many bones possess a weak or absent cerium anomaly (indicative of reducing conditions), and in some bones the trace element composition indicates a local pore water environment equivalent to organic-rich saline waters (Fig. 5).

This study has demonstrated that geochemical taphonomic methods based on comparing the variation in trace element contents of bones from single assemblages developed in terrestrial settings (Trueman, 1999) are also successful in marine environments. Marine environments are relatively homogeneous and thus methods that rely on the development of distinct geochemical signals may have difficulty in resolving distinct taphonomic histories in marine settings. However, this apparent disadvantage must be considered in the context of the relatively poor understanding of taphonomic processes operating the marine realm. Furthermore, homogeneous marine environments are more likely to meet an underlying assumption associated with geochemical taphonomic methods, i.e. that a similar range of potential depositional environments existed during the formation of all assemblages under study.

Geochemical taphonomic methods provide an independent method to establish taphonomic history and isotaphonomic equivalence among vertebrate assemblages, and these techniques should be used together with traditional taphonomic and sedimentary analyses to support palaeoecological, palaeoenvironmental or geochemical inferences on attritional vertebrate accumulations from marine or terrestrial environments.

Acknowledgements

This work was partially supported by a University of Bristol Tratman Scholarship to C.N.T., and NERC grant GR9/01679. Tony Kemp at the Department of Earth Sciences, University of Bristol, provided invaluable help and support with all analytical procedures. The authors would like to thank Kay Behrensmeyer, the editors of Palaeogeogr. Palaeoclim. Palaeoecol., and an anonymous reviewer for valuable comments on earlier versions of the manuscript. Discussions of REE behaviour (Terry Williams, and Eva Valsami-Jones), and bioerosion in bone (Angela Guenery and Lynne Bell) were both valuable and interesting. The authors would also like to thank Steve Howe (NMGW, Cardiff), and Dave Martill (University of Portsmouth) for access to the thin section collection and Heather Jackson (NMGW, Cardiff) for assistance in the field.

References

Altschuler, Z.S., 1980. The geochemistry of trace elements in marine phosphorites. part 1: characteristic abundances and enrichment. In: Bentor, Y.K. (Ed.), Marine Phosphorites. Society of Economic Paleontology and Mineralogy, pp. 18–30.

Behrensmeyer, A.K., Kidwell, S.M., Gastaldo, R.A., 2000. Taphonomy and Paleobiology. Paleobiology 26, 103–147.

Behrensmeyer, A.K., Hook, R.W., 1992. Paleoenvironmental contexts and taphonomic modes. In: Behrensmeyer, A.K., Damuth, J.D., DiMichele, W.A., Potts, R., Dieter Sues, H., Wing, S.L. (Eds.), Terrestrial Ecosystems Through Time. University of Chicago Press, Cicago, IL, pp. 15–136.

Bell, L.S., Skinner, M.F., Jones, S.J., 1996. The speed of post mortem change to the human skeleton and its taphonomic significance. Forensic Sci. Int. 82, 129–140.

Benton, M.J., Cook, E., Turner, P., 2002. Permian and Triassic Red Beds and the Penarth Group of Great Britain. Geol. Conserv. Rev. Ser. 24, Joint Nature Conservation Committee, Peterborough.

Bertram, C.J., Elderfield, H., Aldridge, R.J., Conway Morris, S., 1992. $^{87}Sr/^{86}Sr$, $^{143}Nd/^{144}Nd$ and REEs in Silurian phosphatic fossils. Earth Planet. Sci. Lett. 113, 239–249.

Briggs, D.E.G., Kear, A.J., 1994. Decay and mineralization of shrimps. Palaios 9, 431–456.

Brookins, D.G., 1988. Eh-pH diagrams for geochemistry. Springer, New York, 200 pp.

Casey, R., 1963. Dawn of the Cretaceous. Bull. South East Union Sci. Soc. 117, 1–15.

Clements, R.G., 1993. Type-section of the Purbeck Limestone Group, Durlston Bay, Swanage. Proc. Dorset Nat. Hist. Arch. Soc. 114, 181–206.

Elderfield, H., Greaves, M.J., 1982. The rare earth elements in seawater. Nature 296, 214–219.

Elderfield, H., Pagett, R., 1986. Rare earth elements in ichthyoliths: Variations with redox conditions and depositional environment. Sci. Total Env. 49, 175–197.

Elderfield, H., Sholkovitz, E.R., 1987. Rare earth elements in the pore waters of reducing nearshore sediments. Earth Planet. Sci. Lett. 82, 280–288.

Garrells, R.M., Christ, C.L., 1965. Minerals, Solutions and Equilibria. Harper and Railey, New York.

Girard, C., Albarède, F., 1996. Trace elements in conodont phosphates from the Frasnian/Famennian boundary. Palaeogeogr. Palaeoclim. Palaeoecol. 126, 195–209.

Grandjean, P., Cappetta, H., Michard, A., Albarède, F., 1987. The assessment of REE patterns and $^{143}Nd/^{144}Nd$ ratios in fish remains. Earth Planet Sci. Lett. 84, 181–196.

Grandjean-Lécuyer, P., Feist, R., Albarède, F., 1993. Rare earth elements in old biogenic apatites. Geochim. Cosmochim. Acta 57, 2507–2514.

Hackett, C.J., 1981. Microscopical focal destruction (tunnels) in excavated human bones. Med. Sci. Law. 21, 243–265.

Haq, B.U., Hardenbol, J., Vail, P.R., 1988. Mesozoic and Cenozoic chronostratigraphy and cycles of sea-level change. In: Wilgus, C.K., Hastings, B.S., Kendall, C.G., Posamentier, H.W., Ross, C.A., Van Wagoner, J.C. (Eds.), Sea-Level Changes: An Integrated Approach. Society of Economic Paleontologists and Mineralogists Special Publication, pp. 71–108.

Hedges, R.E.M., Millard, A.R., Pike, A.W.G., 1995. Measurements and relationships of diagenetic alteration of bone from three archaeological sites. J. Arch. Sci. 22, 201–209.

Hubert, J.F., Panish, P.T., Chure, D.J., Prostak, K.S., 1996. Chemistry, microstructure, petrology, and diagenetic model of Jurassic dinosaur bones, Dinosaur National Monument, Utah. J. Sed. Res. 66, 531–547.

Jarvis, I., 1992. Sedimentology, geochemistry and origin of phosphatic chalks: the Upper Cretaceous deposits of NW Europe. Sedimentology 39, 55–97.

MacQuaker, J.H.S., 1994. Palaeoenvironmental significance of 'bone-beds' in organic-rich mudstone successions: an example from the Upper Triassic of south-west Britain. Zool. J. Linn. Soc. 112, 285–308.

McClellan, G.H., Van Kauwenbergh, S.J., 1990. Mineralogy of sedimentary apatites. In: Notholt, A.J.G., Jarvis, I. (Eds.), Phosphorite Research and Development. Geological Society Special Publication, pp. 23–31.

Person, A., Bocherens, H., Mariotti, A., Renard, M., 1996. Diagenetic evolution and experimental heating of bone phosphate. Palaeogeog. Palaeoclim. Palaeoecol. 126, 135–149.

Pfretzschner, H.-U., 2000. Microcracks and fossilization of haversian bone. N. Jb. Geol. Palaont. Abh. 216, 413–432.

Rae, A.M., Ivanovitch, M., 1984. Successful application of uranium series dating of fossil bone. Appl. Geochem. 1, 419–426.

Roux, W., 1887. Uber eine Knochen lebende Gruppe von Faderpilzen (Mycelites ossifragus). Z. Wiss. Zool. 45, 227–254.

Shuffert, J.D., Kastner, M., Emanuele, G., Jahnke, R.A., 1990. Carbonate-ion substitution in francolite: A new equation. Geochim. Cosmochim. Acta 54, 2323–2328.

Staron, R., Granstaff, B., Gallagher, W., Grandstaff, D.E., 2001. REE signals in vertebrate fossils from Sewel, NJ: Implications for location of the K-T boundary. Palaios 16, 255–265.

Storrs, G.W., 1994. Fossil vertebrate faunas of the British Rhaetian (latest Triassic). Zool. J. Linn. Soc 112, 217–259.

Swift, A., Martill, D.M., 1999. Fossils of the Rhaetic. The Palaeontological Association, London, 312 pp.

Sykes, J.H., 1977. British Rhaetian bone-beds. Mercian Geol. 5, 39–48.

Trueman, C.N., 1999. Rare earth element geochemistry and taphonomy of terrestrial vertebrate assemblages. Palaios 14, 555–568.

Trueman, C.N., Benton, M.J., 1997. A geochemical method to trace the taphonomic history of reworked bones in sedimentary settings. Geology 25, 263–266.

Trueman, C.N., Martill, D.M., 2002. The long term preservation of bone: The role of bioerosion. Archaeometry 44, 371–382.

Trueman, C.N., Tuross, N., 2002. Trace elements in modern and ancient bone. In: Kohn, M.J., Rakovan, J., Hughes, J.M. (Eds.), Phosphates – Geochemical, Geobiological and Materials Importance. Rev. Mineral. Geochem. 48, Mineralogical Society of America, Washington, DC. pp. 489–522.

Williams, C.T., Potts, P.J., 1988. Element distribution maps in fossil bones. Archaeometry 30, 237–247.

Wright, J., Seymour, R.S., Shaw, H.F., 1984. REE and Nd isotopes in conodont apatite: variations with geological age and depositional environment. In: Clark, D.L. (Eds.), Conodont Biofacies and Provincialism. Geological Society of America Special Paper, pp. 325–340.

Wright, J.R.L., 1996. Fossil Vertebrate Trackways: Their Origin, Preservation and Significance, PhD thesis. University of Bristol.